Observation of Radiative $B \to \phi K \gamma$ Decays

A. Drutskoy,[8] K. Abe,[4] K. Abe,[33] T. Abe,[4] H. Aihara,[35] M. Akatsu,[17] Y. Asano,[39] V. Aulchenko,[1] T. Aushev,[8] A. M. Bakich,[31] Y. Ban,[26] A. Bay,[13] I. Bedny,[1] P. K. Behera,[40] I. Bizjak,[9] A. Bondar,[1] A. Bozek,[21] M. Bračko,[15,9] T. E. Browder,[3] B. C. K. Casey,[3] Y. Chao,[20] B. G. Cheon,[30] R. Chistov,[8] Y. Choi,[30] A. Chuvikov,[27] M. Danilov,[8] M. Dash,[41] L. Y. Dong,[6] S. Eidelman,[1] V. Eiges,[8] N. Gabyshev,[4] A. Garmash,[1,4] T. Gershon,[4] B. Golob,[14,9] J. Haba,[4] C. Hagner,[41] F. Handa,[34] N. C. Hastings,[4] H. Hayashii,[18] M. Hazumi,[4] L. Hinz,[13] T. Hokuue,[17] Y. Hoshi,[33] W.-S. Hou,[20] H.-C. Huang,[20] Y. Igarashi,[4] T. Iijima,[17] K. Inami,[17] A. Ishikawa,[17] R. Itoh,[4] H. Iwasaki,[4] M. Iwasaki,[35] Y. Iwasaki,[4] H. K. Jang,[29] J. H. Kang,[43] J. S. Kang,[11] P. Kapusta,[21] N. Katayama,[4] T. Kawasaki,[23] H. Kichimi,[4] D.W. Kim,[30] H. J. Kim,[43] Hyunwoo Kim,[11] J. H. Kim,[30] S. K. Kim,[29] K. Kinoshita,[2] P. Koppenburg,[4] S. Korpar,[15,9] P. Križan,[14,9] P. Krokovny,[1] Y.-J. Kwon,[43] S. H. Lee,[29] T. Lesiak,[21] J. Li,[28] J. MacNaughton,[7] D. Marlow,[27] T. Matsumoto,[37] A. Matyja,[21] W. Mitaroff,[7] H. Miyata,[23] D. Mohapatra,[41] G. R. Moloney,[16] T. Mori,[36] T. Nagamine,[34] Y. Nagasaka,[5] T. Nakadaira,[35] E. Nakano,[24] M. Nakao,[4] J.W. Nam,[30] Z. Natkaniec,[21] S. Nishida,[4] O. Nitoh,[38] S. Ogawa,[32] T. Ohshima,[17] S. Okuno,[10] S. L. Olsen,[3] W. Ostrowicz,[21] H. Ozaki,[4] P. Pakhlov,[8] H. Palka,[21] C.W. Park,[11] H. Park,[12] K. S. Park,[30] N. Parslow,[31] M. Peters,[3] L. E. Piilonen,[41] N. Root,[1] H. Sagawa,[4] S. Saitoh,[4] Y. Sakai,[4] T. R. Sarangi,[40] A. Satpathy,[4,2] O. Schneider,[13] J. Schümann,[20] A. J. Schwartz,[2] S. Semenov,[8] K. Senyo,[17] M. E. Sevior,[16] H. Shibuya,[32] B. Shwartz,[1] V. Sidorov,[1] J. B. Singh,[25] N. Soni,[25] S. Stanič,[39,*] M. Starič,[9] A. Sugi,[17] K. Sumisawa,[4] T. Sumiyoshi,[37] S. Suzuki,[42] S. Y. Suzuki,[4] F. Takasaki,[4] N. Tamura,[23] M. Tanaka,[4] Y. Teramoto,[24] T. Tomura,[35] K. Trabelsi,[3] T. Tsuboyama,[4] T. Tsukamoto,[4] S. Uehara,[4] S. Uno,[4] G. Varner,[3] K. E. Varvell,[31] C. H. Wang,[19] J. G. Wang,[41] M.-Z. Wang,[20] Y. Watanabe,[36] E. Won,[11] Y. Yamada,[4] Y. Yamashita,[22] M. Yamauchi,[4] Y. Yuan,[6] Y. Yusa,[34] Z. P. Zhang,[28] V. Zhilich,[1] and D. Žontar[14,9]

(Belle Collaboration)

[1]*Budker Institute of Nuclear Physics, Novosibirsk*
[2]*University of Cincinnati, Cincinnati, Ohio 45221*
[3]*University of Hawaii, Honolulu, Hawaii 96822*
[4]*High Energy Accelerator Research Organization (KEK), Tsukuba*
[5]*Hiroshima Institute of Technology, Hiroshima*
[6]*Institute of High Energy Physics, Chinese Academy of Sciences, Beijing*
[7]*Institute of High Energy Physics, Vienna*
[8]*Institute for Theoretical and Experimental Physics, Moscow*
[9]*J. Stefan Institute, Ljubljana*
[10]*Kanagawa University, Yokohama*
[11]*Korea University, Seoul*
[12]*Kyungpook National University, Taegu*
[13]*Institut de Physique des Hautes Énergies, Université de Lausanne, Lausanne*
[14]*University of Ljubljana, Ljubljana*
[15]*University of Maribor, Maribor*
[16]*University of Melbourne, Victoria*
[17]*Nagoya University, Nagoya*
[18]*Nara Women's University, Nara*
[19]*National Lien-Ho Institute of Technology, Miao Li*
[20]*Department of Physics, National Taiwan University, Taipei*
[21]*H. Niewodniczanski Institute of Nuclear Physics, Krakow*
[22]*Nihon Dental College, Niigata*
[23]*Niigata University, Niigata*
[24]*Osaka City University, Osaka*
[25]*Panjab University, Chandigarh*
[26]*Peking University, Beijing*
[27]*Princeton University, Princeton, New Jersey 08545*
[28]*University of Science and Technology of China, Hefei*
[29]*Seoul National University, Seoul*
[30]*Sungkyunkwan University, Suwon*
[31]*University of Sydney, Sydney NSW*
[32]*Toho University, Funabashi*

 0031-9007/04/92(5)/051801(5)$22.50

[33]Tohoku Gakuin University, Tagajo
[34]Tohoku University, Sendai
[35]Department of Physics, University of Tokyo, Tokyo
[36]Tokyo Institute of Technology, Tokyo
[37]Tokyo Metropolitan University, Tokyo
[38]Tokyo University of Agriculture and Technology, Tokyo
[39]University of Tsukuba, Tsukuba
[40]Utkal University, Bhubaneswer
[41]Virginia Polytechnic Institute and State University, Blacksburg, Virginia 24061
[42]Yokkaichi University, Yokkaichi
[43]Yonsei University, Seoul

(Received 3 September 2003; published 3 February 2004)

The radiative decay $B \to \phi K \gamma$ is observed for the first time. The branching fraction for the charged $B^- \to \phi K^- \gamma$ decay mode is measured to be $\mathcal{B}(B^- \to \phi K^- \gamma) = (3.4 \pm 0.9 \pm 0.4) \times 10^{-6}$. The photon energy distribution for the $B^- \to \phi K^- \gamma$ decay is presented. The signal for the neutral $\bar{B}^0 \to \phi \bar{K}^0 \gamma$ decay mode is not statistically significant and an upper limit, $\mathcal{B}(\bar{B}^0 \to \phi \bar{K}^0 \gamma) < 8.3 \times 10^{-6}$ at 90% C.L., is set. The analysis is based on a data set of 90 fb^{-1} collected by the Belle experiment at the e^+e^- asymmetric collider KEKB.

DOI: 10.1103/PhysRevLett.92.051801 PACS numbers: 13.20.He, 13.25.Hw

Radiative "penguin" B meson decays provide an important tool to search for physics beyond the standard model. Recent experimental studies [1–8] of inclusive and exclusive radiative B decays are in good agreement with standard model predictions [9,10]. New information on radiative B decays is important to further test theoretical models. In this analysis the exclusive decay mode $B \to \phi K \gamma$ is studied for the first time. The experimental techniques used in this analysis are similar to those used in the recently published studies of $B^0 \to K^+ \pi^- \gamma$ and $B^+ \to K^+ \pi^- \pi^+ \gamma$ decays by the Belle Collaboration [3]. Measurement of the branching fraction for the $B \to \phi K \gamma$ decay and its contribution to inclusive radiative $B \to X_s \gamma$ decays is important to constrain theoretical models. Moreover, due to the narrow width of the ϕ resonance, exclusive $B \to \phi K \gamma$ decays are well separated from background and can be effectively used for measurements of the photon momentum over a wide interval. Such measurements can shed some light on the behavior of the photon momentum spectrum in inclusive decays, where the theoretically interesting region below 2 GeV/c is difficult to study experimentally because of large backgrounds. The decay channel $\bar{B}^0 \to \phi \bar{K}^0 \gamma$ can also be used in future high statistics measurements of time-dependent CP violation parameters. With a larger data set, such three-body hadronic final state decays could also be used for angular distribution measurements [11]. The decay $B^- \to \phi K^- \gamma$ (charge conjugate modes are implied throughout this Letter) can be described by conventional radiative penguin diagrams with the creation of an additional $s\bar{s}$ pair (for example, see Fig. 1).

The 90 fb^{-1} data sample containing $(95.8 \pm 0.5) \times 10^6$ produced $B\bar{B}$ pairs was collected with the Belle detector [12] at KEKB [13], an asymmetric energy double-storage-ring collider with 8 GeV electrons and 3.5 GeV positrons. Belle is a general-purpose large-solid-angle detector that consists of a three-layer silicon vertex detector, a 50-layer central drift chamber (CDC), an array of aerogel Čerenkov counters (ACC), a time-of-flight counter system (TOF), and a CsI(Tl) electromagnetic calorimeter (ECL) located inside a superconducting solenoid coil with a 1.5 T magnetic field. An iron flux return located outside the coil is instrumented to identify K_L^0 and muons. The detector is described in detail elsewhere [12]. A detailed GEANT-based simulation of the Belle detector is used to produce Monte Carlo (MC) event samples and determine efficiencies.

Charged tracks with impact parameters less than 2 cm radially and less than 5 cm in z (z axis is antiparallel to the positron beam direction) are used. Kaon and pion mass hypotheses are assigned to charged tracks with a momentum larger than 100 MeV/c, using a likelihood ratio $\mathcal{L}_{K/\pi}$, obtained by combining information from the CDC (dE/dx), ACC, and TOF systems. The likelihood ratio $\mathcal{L}_{K/\pi}$ ranges between 0 and 1 and is required to be larger than 0.8 for the kaon candidates and less than 0.8 for the pion candidates. A relaxed likelihood ratio requirement $\mathcal{L}_{K/\pi} > 0.4$ is applied for the kaon candidates used to reconstruct ϕ mesons.

A candidate primary photon (γ) is required to have an energy E_γ^* in the $\Upsilon(4S)$ center-of-mass (c.m.) frame

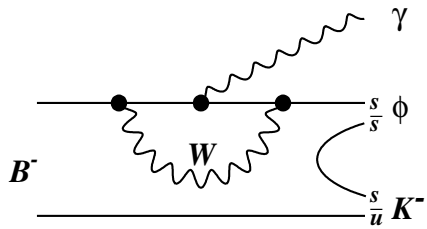

FIG. 1. A "penguin" diagram for $B^- \to \phi K^- \gamma$ with $s\bar{s}$ pair creation.

between 2.0 and 2.7 GeV and to lie within the acceptance of the barrel ECL ($33° < \theta_\gamma < 128°$). The main background sources of high energy photons are $\pi^0 \to \gamma\gamma$ and $\eta \to \gamma\gamma$ decays. To reduce these backgrounds, restrictions are imposed on the invariant mass of the candidate photon and any other photon (γ') in the event. The candidate photon is rejected if $120 < M(\gamma\gamma') < 145$ MeV/c^2 and $E_{\gamma'} > 30$ MeV or if $510 < M(\gamma\gamma') < 570$ MeV/c^2 and $E_{\gamma'} > 200$ MeV. To reduce the background from π^0 decays when the two daughter photons form a single cluster in the calorimeter, the ratio of the energy deposition in 3×3 ECL cells compared to that in 5×5 cells around the maximum energy ECL cell is required to exceed 95%.

The K_S^0 candidates are formed from $\pi^+\pi^-$ combinations that have an invariant mass within ± 10 MeV/c^2 of the nominal K_S^0 mass ($\sim 3\sigma$ in the K_S^0 mass resolution). The two pions are required to have a common vertex that is displaced from the interaction point by more than 0.5 cm in the plane perpendicular to the beam direction. The difference in z coordinates for the tracks constituting the secondary vertex must be less than 2 cm. The angle α between the K_S^0 flight direction and the measured K_S^0 momentum direction is required to satisfy $\cos\alpha > 0.8$. Oppositely charged K mesons are combined to form ϕ candidates; their invariant mass is required to be within ± 10 MeV/c^2 ($\sim 3\sigma$) of the nominal value for the ϕ mass.

The $\phi K^-\gamma$ and $\phi \bar{K}_S^0 \gamma$ combinations are selected to form B^- and $\bar{B}^0$ candidates. Two kinematic variables are used to extract the B meson signal: the energy difference $\Delta E = E_B^* - E_{\rm beam}^*$ and the beam-constrained mass $M_{\rm bc} = \sqrt{(E_{\rm beam}^*)^2 - (p_B^*)^2}$, where E_B^* and p_B^* are the c.m. energy and momentum of the B candidate and $E_{\rm beam}^*$ is the c.m. beam energy. The events that satisfy loose requirements $M_{\rm bc} > 5.2$ GeV/c^2 and $|\Delta E| < 0.4$ GeV are selected for further analysis.

With these selection criteria, the primary background source is continuum $e^+e^- \to q\bar{q}$ production, where q may be a u, d, s, or c quark. To separate spherical $B\bar{B}$ events from jetlike continuum events, a Fisher discriminant is formed from six modified Fox-Wolfram moments [1,14]. Signal and background probability density functions (PDF) for the Fisher discriminant and the cosine of the B flight direction with respect to the z axis ($\cos\theta_B^*$) are obtained from signal MC and sideband data. The signal (background) PDFs are multiplied to form a signal (background) likelihood $\mathcal{L}_S$ ($\mathcal{L}_{\rm BG}$). The likelihood ratio $\mathcal{LR} = \mathcal{L}_S/(\mathcal{L}_S + \mathcal{L}_{\rm BG})$ is required to be greater than 0.3. This event topology requirement retains 92% of the signal events while removing 55% of the continuum events. Finally, the ratio of the second to the zeroth Fox-Wolfram moment, calculated using all particles in the event, is required to be less than 0.5.

Signal MC studies of the ΔE distribution indicate that the width is dominated by photon energy smearing, and the shape is expected to be asymmetric due to photon energy leakage. The resolution in $M_{\rm bc}$ of 3.2 MeV/c^2 is dominated by the beam energy spread of KEKB and is slightly improved to 3.0 MeV/c^2 by rescaling the photon energy so that $\Delta E = E_\phi^* + E_K^* + E_\gamma^* - E_{\rm beam}^* = 0$, where E_ϕ^* and E_K^* are ϕ meson and K meson energies in the c.m. frame.

The $M_{\rm bc}$ distribution for the interval $-0.08 < \Delta E < 0.05$ GeV and the ΔE distribution for the interval $5.27 < M_{\rm bc} < 5.29$ GeV/c^2 for $B^- \to \phi K^-\gamma$ decay mode are shown in Figs. 2(a) and 2(b). To avoid systematic uncertainties that could arise from the description of the ΔE distribution, the signal yield is extracted from a fit of the $M_{\rm bc}$ distribution after applying the asymmetric cut $-0.08 < \Delta E < 0.05$ GeV. The $M_{\rm bc}$ distribution is fitted to the sum of a Gaussian function and the so-called

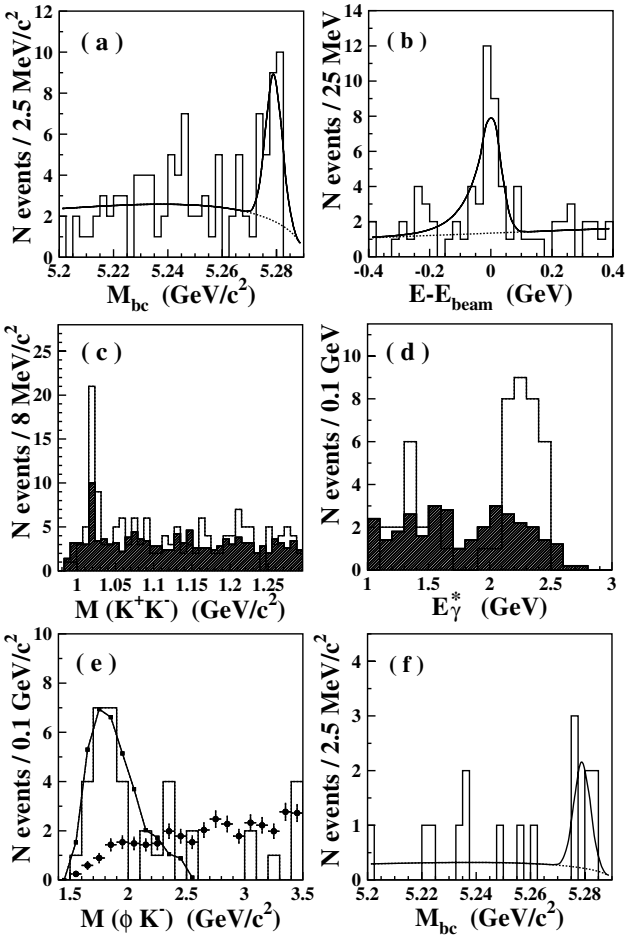

FIG. 2. The (a) $M_{\rm bc}$, (b) ΔE, (c) $M(K^+K^-)$, (d) E_γ^*, and (e) $M(\phi K^-)$ distributions for the $B^- \to \phi K^-\gamma$ decay mode and the (f) $M_{\rm bc}$ distribution for the $\bar{B}^0 \to \phi \bar{K}^0 \gamma$ decay mode are shown by histograms. The solid histograms are obtained with events from the B mass sideband. The curves show the results of the fit described in the text. The measured $M(\phi K^-)$ distribution is compared to those obtained from the MC simulation, with a three-body phase-space model (circles with error bars) or adjusted to follow the data (squares connected by a line).

ARGUS background function [15]. The width of the signal Gaussian is determined from MC data, while the peak position is fixed to 5.279 GeV/c^2. The background shape was studied using $M_{\rm bc}$ and ϕ mass sidebands and found to be flat. The fitted number of B candidates is $N = 21.6 \pm 5.6$. As a cross-check, the ΔE distribution was fitted with the Crystal Ball line shape function [16] (the shape is fixed from MC data) to describe the signal and a linear function to describe the background. The signal yield is $N = 23.6 \pm 5.4$ events, which is consistent with the $M_{\rm bc}$ fit result. The K^+K^- mass distribution with two combinations per event is shown in Fig. 2(c) for events in the B signal region, $5.27 < M_{\rm bc} < 5.29$ GeV/c^2 and $-0.08 < \Delta E < 0.05$ GeV. The solid histogram in Fig. 2(c) shows events from the B meson mass sideband, $5.2 < M_{\rm bc} < 5.26$ GeV/c^2, with a normalization obtained from the $M_{\rm bc}$ distribution fit.

The photon energy distribution for the $B^- \to \phi K^- \gamma$ decay channel for events within the B signal region with an extended photon energy interval $1.0 < E^*_\gamma < 3.0$ GeV is shown in Fig. 2(d). The solid histogram shows events from the B mass sideband, which are used to describe the background. The MC determined B meson reconstruction efficiency is nearly constant for photon energies between 1.5 and 2.7 GeV. Figure 2(d) demonstrates that the signal events are concentrated in the range $2.1 < E^*_\gamma < 2.5$ GeV, and events outside that range are consistent with background, estimated from the B mass sideband events. The bulk of inclusive $B \to X_s\gamma$ events was also observed in the $E^*_\gamma > 2.0$ GeV range [1,4,6]. According to the theoretical calculation of the radiative "penguin" decay processes [17], 90% or more of the $B \to X_s\gamma$ events are expected to lie in the $E^*_\gamma > 2.0$ GeV range. A similar fraction is also expected in the photon energy distribution for the $B^- \to \phi K^- \gamma$ decays. The maximum photon energy is kinematically constrained by the mass of the hadronic system and is therefore slightly lower in $B^- \to \phi K^- \gamma$ decays compared to $B \to X_s\gamma$.

To search for a possible contribution from kaonic resonances decaying to ϕK^-, the ϕK^- invariant mass distribution is also shown in Fig. 2(e). This distribution is strongly correlated with the photon energy distribution. Background was not subtracted in Fig. 2(e) because of the small number of signal and background events. Events mostly populate the low-mass range; however, the small data sample precludes any definite conclusions. It is clear that the observed ϕK^- mass distribution differs significantly from that in the three-body phase-space decay [also shown in Fig. 2(e)]. To provide the correct branching fraction measurement, the MC data sample was adjusted to follow the measured ϕK^- invariant mass distribution.

The $M_{\rm bc}$ distribution for the $\bar{B}^0 \to \phi \bar{K}^0 \gamma$ decay channel is shown in Fig. 2(f). The figure is obtained in a similar manner to those for $B^- \to \phi K^- \gamma$ decay. In the fit of the $M_{\rm bc}$ distribution the peak position is fixed to the value 5.279 GeV/c^2 and the background shape (defined by the slope parameter of the ARGUS function) is constrained to be flat.

The signal yields, efficiencies, branching fractions, and significances obtained for the $B^- \to \phi K^- \gamma$ and $\bar{B}^0 \to \phi \bar{K}^0 \gamma$ decay channels for the photon energy range $2.0 < E^*_\gamma < 2.7$ GeV are given in Table I. The signal in the decay channel $B^- \to \phi K^- \gamma$ has a 5.5σ significance, whereas that for $\bar{B}^0 \to \phi \bar{K}^0 \gamma$ is 3.3σ and a 90% confidence level upper limit, which is calculated assuming a Gaussian distribution of the statistical error, and an additional one unit of the systematic error contribution is also given. The statistical significance is defined as $\sqrt{-2\ln(\mathcal{L}_0/\mathcal{L}_{\rm max})}$, where $\mathcal{L}_{\rm max}$ and $\mathcal{L}_0$ are likelihood values at the best-fit signal yield and the signal yield fixed to zero. The branching fractions for the decays of the intermediate ϕ and $\bar{K}^0$ states are taken from Ref. [18] and are not included in the efficiencies quoted in Table I. No event with more than one B candidate is found in the data; the double counting probability for the $B^- \to \phi K^- \gamma$ channel is estimated by MC data to be $(1.2 \pm 0.3)\%$ and is accounted for in the efficiency calculation. An equal production rate for the neutral and charged B mesons is assumed, and the uncertainty ($\sim$7%) related to this assumption [18] is not included in the total systematic error.

In addition to the dominant continuum background, various $B\bar{B}$ background sources were studied. The only significant background found, with a contribution exceeding 1% of the signal level, arises from nonresonant $B^- \to K^-K^-K^+\gamma$ decays. This contribution is estimated to be $(4 \pm 4)\%$ using events from the high mass ϕ meson sideband $1.05 < M_{K^+K^-} < 1.25$ GeV/c^2. The shape of this background as a function of $M_{K^+K^-}$ is taken from the MC simulation, assuming nonresonant decay $K^{*-}(1770) \to K^-K^-K^+$. The $B^- \to \phi K^- \gamma$ branching fraction is corrected for this contribution, and the uncertainty is included in the systematic error.

TABLE I. The signal yields obtained from the $M_{\rm bc}$ fit, efficiencies, branching fractions, upper limit, and significances for the $B^- \to \phi K^- \gamma$ and $\bar{B}^0 \to \phi \bar{K}^0 \gamma$ decay modes.

Decay mode	Yield	Efficiency (%)	Branching fraction (10^{-6})	Significance (σ)
$B^- \to \phi K^- \gamma$	21.6 ± 5.6	12.9	$3.4 \pm 0.9 \pm 0.4$	5.5
$\bar{B}^0 \to \phi \bar{K}^0 \gamma$	5.8 ± 3.0	7.9	$4.6 \pm 2.4 \pm 0.6$	3.3
			<8.3 (90% C.L.)	

The major sources contributing to the systematic uncertainty of the branching fraction measurements are the photon reconstruction efficiency and energy scale (4%), the reconstruction efficiency of charged tracks (1% per track), the charged kaon particle identification (1% per particle), the neutral kaon reconstruction efficiency (3%), uncertainties in the nonresonant background under the ϕ signal (4%), uncertainties in the angular distributions applied in the MC simulation of the hadronic states (5%), uncertainties in the MC simulation of π^0 and η rejection criteria (2%), uncertainty in the efficiency of the topological likelihood cut (2%), uncertainties of the background and B signal shape description in the fit (5%), and uncertainty in the determination of the number of $B\bar{B}$ pairs ($<1\%$). The systematic uncertainties described above are added in quadrature to obtain the final systematic errors.

In conclusion, the $B \to \phi K \gamma$ decay modes were studied for the first time. A branching fraction for the $B^- \to \phi K^- \gamma$ decay mode and an upper limit for the $\bar{B}^0 \to \phi \bar{K}^0 \gamma$ decay mode were obtained. The measured $B^- \to \phi K^- \gamma$ decay branching fraction is roughly an order of magnitude smaller than the $B \to K^* \gamma$ branching fractions. This factor can be attributed to the creation of the additional $s\bar{s}$ pair. Signal events are concentrated in the photon energy range $2.1 < E_\gamma^* < 2.5$ GeV, which is similar to the photon energy range for two-body radiative decays.

We wish to thank the KEKB accelerator group for the excellent operation of the KEKB accelerator. We acknowledge support from the Ministry of Education, Culture, Sports, Science, and Technology of Japan and the Japan Society for the Promotion of Science; the Australian Research Council and the Australian Department of Education, Science and Training; the National Science Foundation of China under Contract No. 10175071; the Department of Science and Technology of India; the BK21 program of the Ministry of Education of Korea and the CHEP SRC program of the Korea Science and Engineering Foundation; the Polish State Committee for Scientific Research under Contract No. 2P03B 01324; the Ministry of Science and Technology of the Russian Federation; the Ministry of Education, Science and Sport of the Republic of Slovenia; the National Science Council and the Ministry of Education of Taiwan; and the U.S. Department of Energy.

*On leave from Nova Gorica Polytechnic, Nova Gorica.

[1] Belle Collaboration, K. Abe *et al.*, Phys. Lett. B **511**, 151 (2001).
[2] Belle Collaboration, K. Abe *et al.*, Contributed Paper, Report No. BELLE-CONF-0319, 2003.
[3] Belle Collaboration, S. Nishida *et al.*, Phys. Rev. Lett. **89**, 231801 (2002).
[4] CLEO Collaboration, S. Chen *et al.*, Phys. Rev. Lett. **87**, 251807 (2001).
[5] CLEO Collaboration, T. E. Coan *et al.*, Phys. Rev. Lett. **84**, 5283 (2000).
[6] BaBar Collaboration, B. Aubert *et al.*, hep-ex/0207076.
[7] BaBar Collaboration, B. Aubert *et al.*, Phys. Rev. Lett. **88**, 101805 (2002).
[8] ALEPH Collaboration, R. Barate *et al.*, Phys. Lett. B **429**, 169 (1998).
[9] See A. Ali, CERN Report No. CERN-TH-2002-284, 2002 (hep-ph/0210183), and references therein.
[10] See T. Hurth, Rev. Mod. Phys. **75**, 1159 (2003), and references therein.
[11] M. Gronau *et al.*, Phys. Rev. Lett. **88**, 051802 (2002).
[12] Belle Collaboration, A. Abashian *et al.*, Nucl. Instrum. Methods Phys. Res., Sect. A **479**, 117 (2002).
[13] S. Kurokawa and E. Kikutani, Nucl. Instrum. Methods Phys. Res., Sect. A **499**, 1 (2003).
[14] G. C. Fox and S. Wolfram, Phys. Rev. Lett. **41**, 1581 (1978).
[15] ARGUS Collaboration, H. Albrecht *et al.*, Phys. Lett. B **229**, 304 (1989).
[16] M. Oreglia, Ph.D. thesis, Stanford University (SLAC Report No. SLAC-236, 1980).
[17] A. L. Kagan and M. Neubert, Eur. Phys. J. C **7**, 5 (1999).
[18] Particle Data Group, K. Hagiwara *et al.*, Phys. Rev. D **66**, 010001 (2002).